Inverse Problems in Science and Engineering
Vol. 15, No. 2, March 2007, 151–162

Taylor & Francis
Taylor & Francis Group

Transducer shape optimization for instability control of smart piezolaminated columns

ABHIJIT MUKHERJEE*, SHAILENDRA P. JOSHI and ARUP SAHA CHAUDHURI

Department of Civil Engineering, Indian Institute of Technology Bombay Powai, Mumbai – 400076, India

(*Received 10 January 2005; in final form 10 October 2005*)

In this article, we present an evolutionary technique to optimize the shape of piezoelectric transducers in order to extend the instability limits of laminated composite columns. A C_o-continuous eight-node plate finite element with five degrees of freedom is employed. An evolutionary shape design procedure based on the residual voltages is developed. It aims at minimizing the quadratic measure of global displacement residual error between the desired and the current structural configuration. The use of evolutionary technique makes the present procedure computationally efficient. It also alleviates the possibility of *checkerboard* solutions that are difficult to interpret and manufacture. The performance of the design is demonstrated in modal control of a cantilever beam and control of a tip loaded cantilever column.

Keywords: Shape optimization; Transducers; Piezoelectric materials; Instability; Compression members; Structural control

1. Introduction

Recent technological advances in the field of material science, microelectronics, and structural analysis and design have led to research in the development of high-performance structures that are light, energy efficient and autonomous, known as *smart structures*. These structures have embedded smart materials that are capable of sensing the undesired changes and applying remedial forces to control the change. Vibration suppression, shape control and instability control are some of the key applications of the smart structures technology. The actuation can be controlled either by optimal distribution of the smart material or by optimal voltage distribution. In this article, we demonstrate a technique for optimum shape design of sensors and actuators control of plate type structures. The techniques for placement of sensors and actuators vary from numerical techniques [1,2], mathematical optimization [3] to heuristic and evolutionary techniques [4,5]. Most attempts at optimal sensing and actuation have been for beam

*Corresponding author. E-mail: abhijit@civil.iitb.ac.in

Inverse Problems in Science and Engineering
ISSN 1741-5977 print/ISSN 1741-5985 online © 2007 Taylor & Francis
http://www.tandf.co.uk/journals
DOI: 10.1080/17415970600872920

structures. In such structures, it is possible to intuitively design the shape of the actuators and sensors that is very close to optimum. In the case of plate structure, an intuitive design is far more difficult, if not impossible. The present article demonstrates a novel technique for the adaptive shape design of actuator and sensor profiles. The elegance of the present method is that it is universal, i.e., it can be applied for any structure with any form of external excitation. A gradientless procedure based on the residual voltages is developed. It aims at minimizing the quadratic measure of global displacement residual error between the desired and the current structural configuration. The actuators gradually adapt to a shape that is most efficient in controlling the structure. The present optimization technique is computationally economical and also avoids *checkerboard* designs that may be difficult to interpret and implement in practice.

2. Transducer shape design

In this section, we present the iterative algorithm for adaptive design of sensor and actuator profiles. The present design method can be applied for static as well as dynamic cases. In static analysis, the objective is to determine the actuator profile that would be efficient in obtaining the desired shape of the structure after it has deformed under external forces. In dynamic analysis, the sensor or the actuator configurations corresponding to the mode shapes that are to be observed or excited are determined. It is to be noted that a reciprocal relationship exists between the sensor and the actuator. Therefore, the shape of the sensor that observes a particular mode (modal sensor) is also the shape of the actuator that excites that mode (modal actuator). The present iterative procedure can therefore be employed in designing both modal sensors and actuators. The objective is to minimize the quadratic measure of the residual deviation of the current deformations of the structure from its desired state. The objective function is thus defined as

$$\min\left[\int \left\{\delta_i(p_1, A_1, \ldots, p_n, A_n) - \delta_0\right\}^2 \mathrm{d}A\right] \tag{1}$$

where,

$\delta_i =$ Normalized deformation vector in ith iteration.
$A_i, \ldots, A_n =$ Areas of actuators that are switched on.
$(p_1, \ldots, p_n) =$ Actuator position vector.
$\delta_0 =$ Normalized desired deformation vector.

The step-by-step procedure for the solution is described subsequently,

1. The entire structural domain is discretized using a fine finite element (FE) mesh.
2. In the case of static analysis, the deformation vector is the solution obtained after analyzing the structure for external mechanical loads. In the dynamic analysis, the mode shape for which the sensor/actuator profile is to be obtained is the deformation vector. Using sensor relation, the voltage in each element (V_s^e) is calculated.
3. The shape design process begins with a maximal *seed* design in that all actuators are switched on. The process continues towards shape determination by *killing* the undesired actuators.

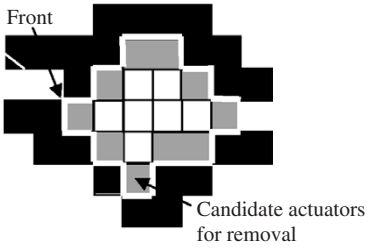

Figure 1. Front growth.

To begin the process of removal of actuators a novel concept of *front opening* is implemented (figure 1). The front is defined by the physical boundaries of the structure. The actuators that lie on the front are removed from the locations of minimal absolute curvature. This is termed as front opening. The actuators that surround the front are candidates for state change.

4. The structure is analyzed based on the current actuator configuration under unit voltage and the voltages developed due to current actuator configuration are calculated (V_a^e).
5. The voltages V_a^e and V_s^e are normalized with respect to their maximum values.

$$\bar{V}_s^e = \frac{V_s^e}{(V_s^e)_{\max}} \quad \bar{V}_a^e = \frac{V_a^e}{(V_a^e)_{\max}} \tag{2}$$

The residual voltages (V_r^e) for the elements on the front are determined as,

$$V_r^e = \left(\bar{V}_s^e - \bar{V}_a^e\right) \tag{3}$$

The elements that have negative residuals are potential actuators to be removed. In practice, a predetermined fraction of these actuators are removed.

6. The quadratic measure of the global residual deviation (α) in deformation is calculated as,

$$\alpha = \sum_{i=1}^{ndof} (\delta_i - \delta_0)^2 \tag{4}$$

7. Steps 4–6 are repeated till the value of α is acceptably small.

3. Numerical examples

In this section, we present the results for both static as well as dynamic cases. Table 1 contains the properties of the plate and the piezoelectric material for all the examples.

3.1. *Example 1: Cantilever plate subjected to uniform pressure*

A long cantilever plate, (0.1 m × 0.02 m), is subjected to a unit edge load. The objective is to find out the actuator layout that gives the original undeformed shape under the given load. Using symmetric boundary conditions, only half the structure is modeled

Table 1. Material properties.

Property	Poly vinylidene fluoride (PVDF)	Aluminum
Young's modulus (GPa), E_1, E_2	2.0, 2.0	70.0
Poisson's ratio, ν_{12}	0.30	0.25
Shear modulus (GPa), G_{12}	0.775	28.00
Piezoelectric strain constant, $C\,m^{-2}$, $e_{31} = e_{32}$	−0.046	–
Thickness (mm)	0.50	1.0
Number of layers	2 (at top and bottom)	1
Density ($N\,s\,m^{-4}$)	1800	2700

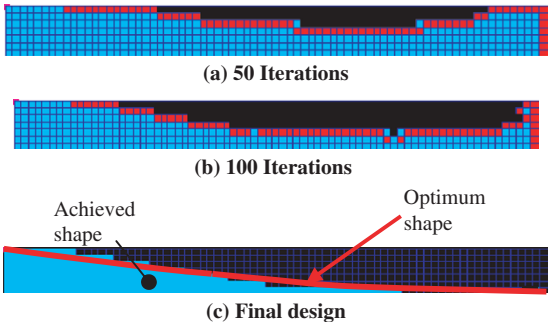

Figure 2. Actuator design history.

with a 75×7 FE mesh. The piezoelectric effect e_{32} is neglected in order to compare the result with one-dimensional solutions. Of the total number of actuators that lie on the front, two actuators that satisfy the condition equation (3) explained in the design procedure are removed in each iteration. Figure 2(a)–(c) shows the different stages in the actuator shape determination. The global error in displacement reduces monotonically till the minimum value is reached (figure 3). Beyond this point any further removal leads to increase in the error.

3.2. *Example 2: Modal transducers*

The first two natural frequencies and the corresponding mode shapes for the cantilever plate in example 1 are obtained by free vibration analysis. The mode shapes are then fed to the optimization routine. In both the cases, the piezoelectric effect in the shorter direction is neglected. Figure 4 shows the intermediate and final profiles corresponding to the first mode.

To examine the efficacy of the design, the structure is subjected to external excitation of nature $f = f_o$ (A sin $\omega_1 t$ + B sin $\omega_2 t$), where A and B are the constants and ω_1 and ω_2 are the forcing frequencies close to the first two natural frequencies of the system. A fast Fourier transform (FFT) of the signal generated by the sensor optimized for the first mode (figure 5) shows only one peak at the first frequency. Thus, the sensor filters out the second mode successfully.

Figure 6(a)–(c) shows the sensor profiles at various stages of the design process for the second mode. Due to changing curvature, the transducer has opposite polarities on

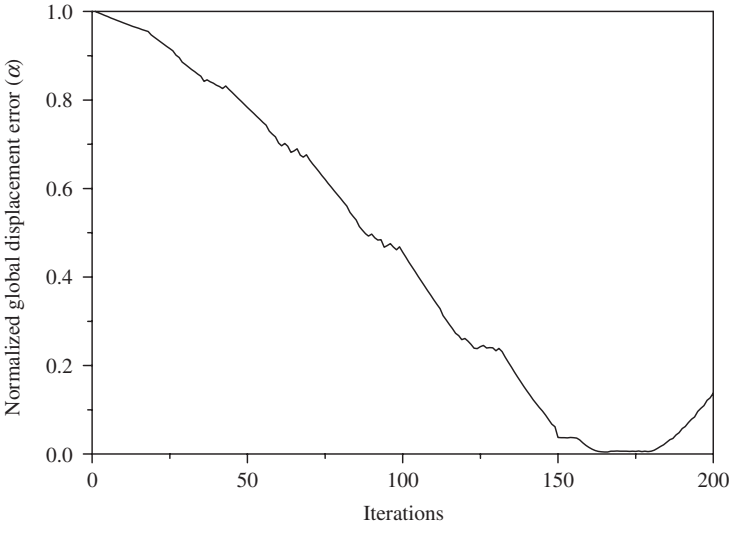

Figure 3. Error history (example 1).

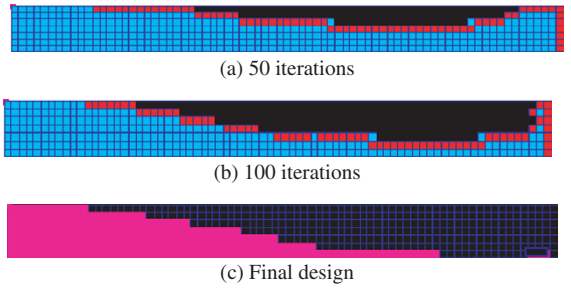

Figure 4. Design history for mode 1 transducer (example 2).

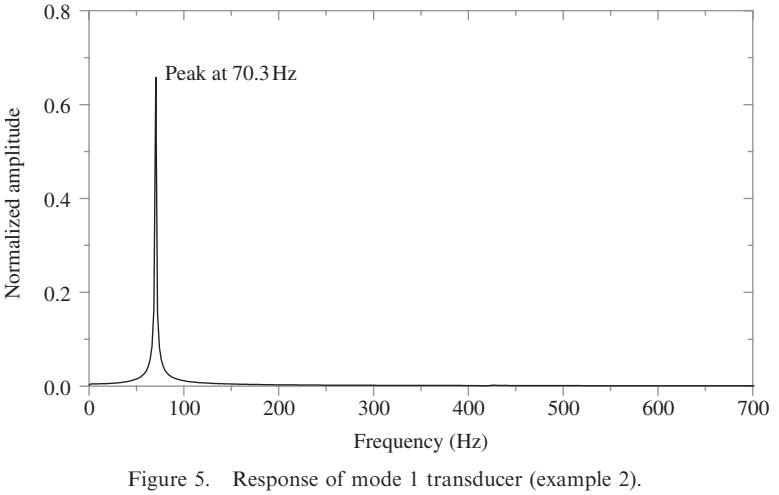

Figure 5. Response of mode 1 transducer (example 2).

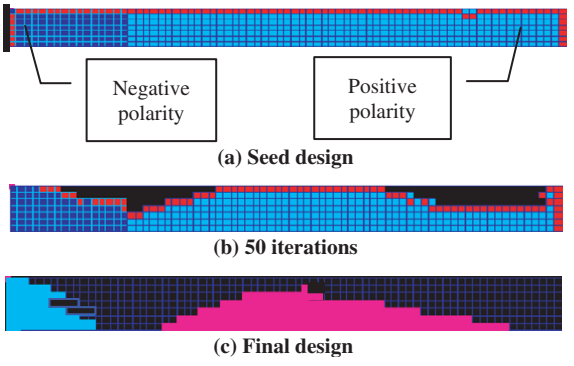

Figure 6. Design history mode 2 transducer (example 2).

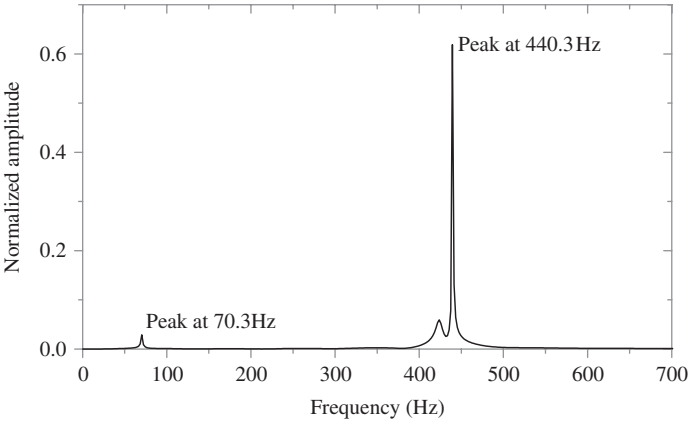

Figure 7. Response of mode 2 transducer (example 2).

either side of the line of contraflexure. The efficacy of the sensor shape is found out by using this shape in detecting the signal from the system under the influence of the forcing function described earlier. It is seen from figure 7 that the transducer optimized for mode 2 responds predominantly in the second mode.

4. Experimental validation

To validate the theory, the experiments have been carried out in three phases. Initially, sensing and actuation of the PVDF layer is tested separately. Finally, active control of cantilever columns is tested using the collocated sensors and actuators. We describe the last phase of the experiment here.

4.1. *Test specimen and experimental setup*

A cantilever column (200 mm × 30 mm × 1.10 mm) made of plastic is used as a test sample (table 2). PVDF sheet manufactured by M/S Measurements Specialists Inc.

is used for fabricating the transducers. The thickness of the sheet is 28 μm. The PVDF sheet is metallized with silver ink on either side that acts as electrodes. The properties of the PVDF sheet are furnished in table 1. The sheet is shaped to fabricate four modal transducers corresponding to the first mode (figure 4). It may be noted that there would be a marginal change in the shape of the modal transducers with the variation of the tip load. However, that effect is neglected here. The shape of the modal transducers is etched on the PVDF sheet. Before the etching process begins, masks of the shape of the required design are adhesively bonded to the sheet. The electrode is removed using acetone as the etching solution, and then the sheet is cut into the desired shape. Etching prevents short-circuiting at the time of cutting the sheet. As the charge is collected only between the overlapped areas of the electrodes, only one side of the sheet is etched leaving the other side intact. Some extra lengths of the PVDF sheet are provided for electrical connection. This area is not bonded to the substrate and metal lugs are attached there for electrical connection. Two such collocated sheets (one overlapped on the other) are applied on each face of the substrate. One acts as sensor while the other acts as actuator. The resulting layup is a balanced symmetric one. When subjected to base oscillation the specimen would undergo pure bending and no resultant inplane or torsional deformation would be present. Such a motion would produce the same magnitude of tensile and compressive strains in the sensors on the opposite sides of the substrate. As a result, electrical charge of the same magnitude but of opposite polarities would be generated on the two sensors. The electrodes on the opposite faces of the sensors are connected to collect the charges from the sensors. Similarly, electrical field of the same magnitude but of opposite polarity is applied on the two actuators to create pure bending in the column. It may be noted that the compressive strain in the column due to its own mass and the tip mass is negligible in comparison to the strains produced due to bending.

The experimental setup is shown in figure 8. It consists of three units – sensing, actuation, and response monitoring. The sensing block consists of the exciter, the specimen, and the sensors. The actuation block consists the signal generator, the gain controller, and the actuators. To control the structure the input signal from the sensors has been used. The gain is controlled through a set of charge amplifiers. The amplifiers accept a maximum input of ± 10 V and maximum output of ± 200 V. As a result, the maximum gain was limited to 20. To monitor the tip displacement a laser distance sensor is used. The signal of the laser sensor is viewed on a FFT analyzer.

Figure 9 shows the flow diagram for sensing, actuation, and monitoring sections. In this article, we shall discuss only the enhancement of damping through active control (active damping).

Table 2. Properties of Plastic and PVDF sheets.

Properties	Plastic	PVDF
Elastic constant (GPa)	5.358	2.0
Poisson's ratio	0.3	0.29
Density ($\mathrm{kg\,m^{-3}}$)	1100	1800
Piezoelectric constant		-23×10^{-12}
Dielectricity, ξ_{33} ($10^{-9}\,\mathrm{F\,m^{-1}}$)		0.1062
Maximum operating voltage ($\mathrm{V\,\mu m^{-1}}$)		30

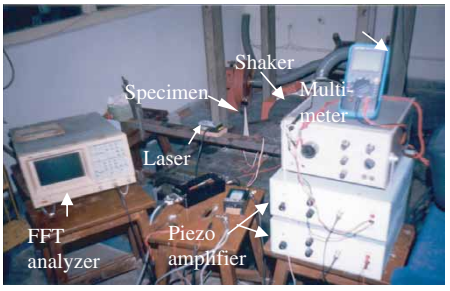

Figure 8. Experimental setup.

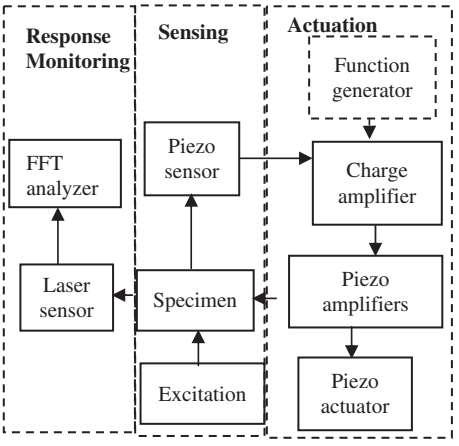

Figure 9. Flow diagram.

4.2. *Active damping*

In this experiment, we demonstrate the control of vibration of the cantilever column by increasing its damping capacity using collocated sensors and actuators. The base excitation is produced by securing the base of the cantilever column on to a shaker (figure 8). The shaker can produce oscillations in the horizontal direction in the range 3 Hz–10 kHz. The shaker is operated until a steady state response of the structure is achieved. The shaker is then stopped suddenly and the attenuation of vibration of the column is noted.

The velocity feedback control algorithm is used here to increase the active damping in the system. The voltage sensed by the sensors is amplified to a specified gain level through a charge amplifier and a piezo amplifier that are connected in series. The resulting voltage is applied to the actuator layer to control the vibration of the column.

In velocity feedback method, the increased active damping is observed in the experiments for tip mass to column mass ratio of 0 to 1.42. The vibration of the active system attenuated quicker than that in the passive one. The effective damping coefficients of the active system have been calculated. It may be noted that active damping can be controlled by controlling the gain only. Therefore, the gain applied

Table 3. Active damping coefficients.

	Applied gain		Damping coefficient (% of critical damping)		
Tip mass (gm)	Experiment	Theory	Structural	Augmented	Ratio
0.0	400	407	4.85	6.70	1.381
3.02	375	384	4.70	6.40	1.361
6.04	350	331	5.00	6.60	1.320
10.36	300	300	5.15	6.70	1.300

corresponding to each damping coefficient is noted. In the present setup, the gain can be controlled to a resolution of 1 V. From the theoretical work, the required gains to achieve the same damping coefficients are evaluated. The theory is validated by comparing the experimental and theoretical gains (table 3). The theoretical and experimental gain values match within an accuracy of 5%.

In figure 10, the attenuation of vibration for different tip loads are shown. Both unactuated and actuated results are furnished. The results are validated with the exact solutions [6].

It can be seen that the theory and the experiment compare very well for all the cases studied here. A more detailed discussion on the experiment is available in [6].

The variation of the active damping coefficient with gain is studied. In figure 11, the attenuation of vibration due to different gains are shown for 6.04 gm tip mass.

From the above figures, the active damping can be calculated for various gains. It is shown in table 4. It can be seen that there has been monotonic increase of effective damping with the increase in the gain. It may be noted that the lower stiffness of PVDF dictated us to use the softer, plastic substrate. The substrate has high material damping. Therefore, the effect of active damping is not predominant. For stiffer substrates with stiffer active materials such as lead zirconate titanate (PZT) the effect should be more predominant.

5. Conclusions

In this article, a gradientless technique to optimize the distribution of piezoelectric transducers for efficient control of plates has been presented. The present design procedure is simple and can easily be integrated with the existing FE tools. A novel concept of front has been developed that makes the design process computationally faster as only the transducers on the front are the candidates for state change. It also eliminates the checkerboard patterns of the sensors/actuators, which are difficult to interpret. The method is universal; i.e., it can be applied to any structure with any external excitation. Several numerical examples demonstrate the efficacy of the design procedure. It is also shown that modal sensors and actuators can be constructed using the present design technique.

The transducers have been employed in vibration control of piezolaminated columns with tip masses. There is a good agreement between theory and the experiments. The columns are made of plastic substrates and PVDF skins. The PVDF skins consist of two layers of PVDF sheets with metallized top and bottom surfaces. Individual layers function as collocated sensors and actuators. The sensors are connected to the actuators

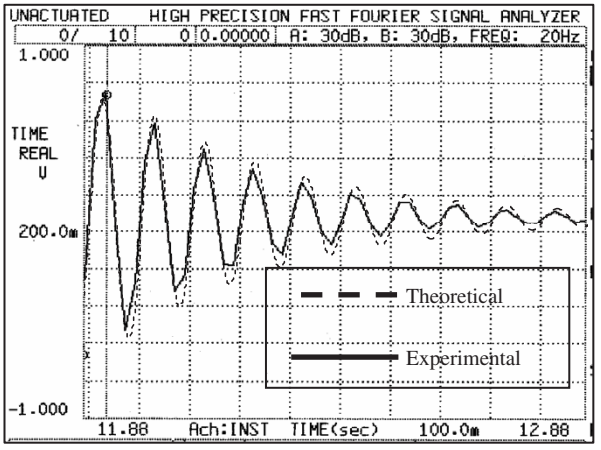

(a) Unactuated

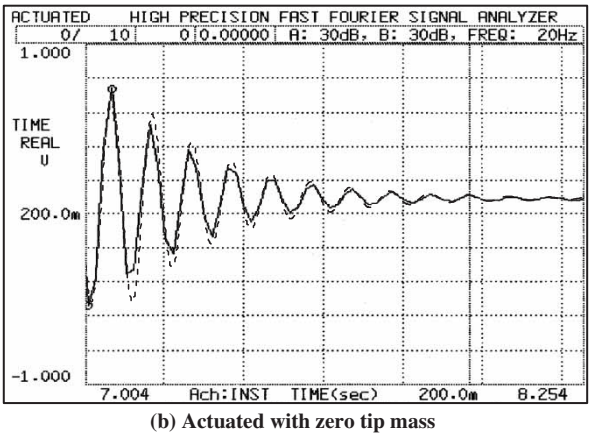

(b) Actuated with zero tip mass

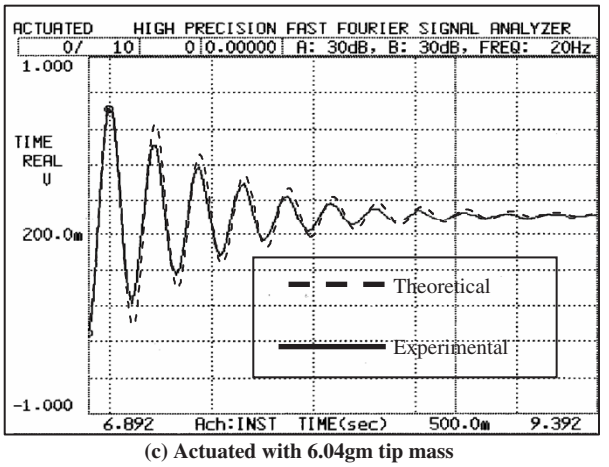

(c) Actuated with 6.04gm tip mass

Figure 10. Theoretical and experimental responses with different tip masses.

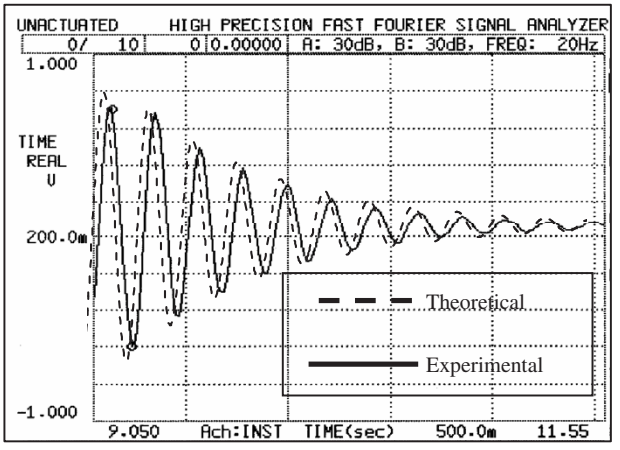

(a) Unactuated

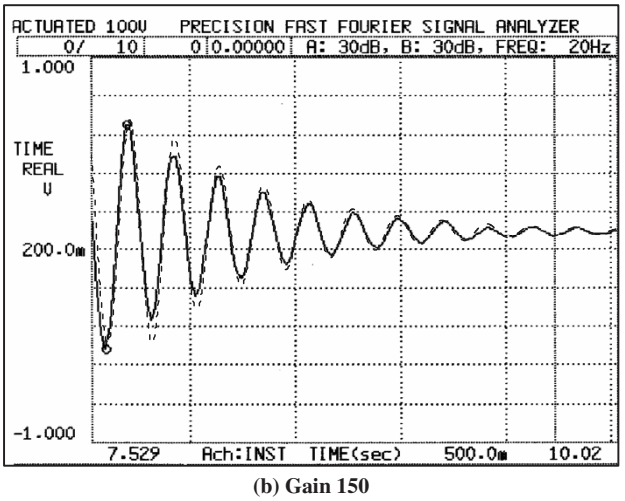

(b) Gain 150

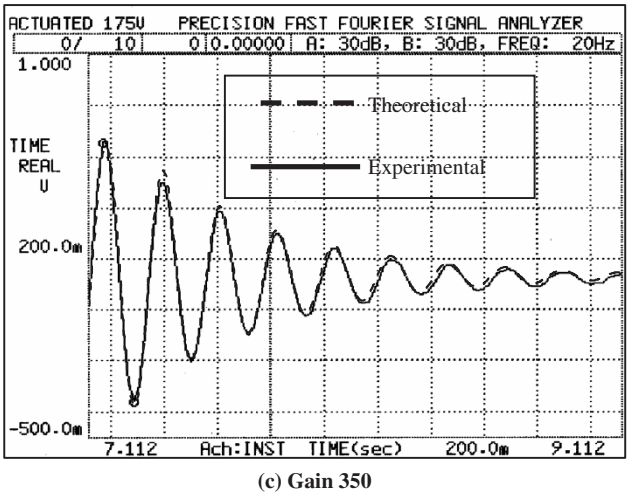

(c) Gain 350

Figure 11. Response with varying gains.

Table 4. Variation of active damping with gain.

Applied gain (approximately)	Damping co-efficient (%)
0	5.00
075	5.35
150	5.70
225	6.00
350	6.60

through a gain control device. A velocity feedback control strategy that augments the damping of the structure is employed. Due to increased damping the vibration attenuates more rapidly. The active damping in the structure can be controlled by controlling the gain multiplier. The experiments demonstrated the efficacy of the piezoelectric materials in vibration control of column structures.

The increased tip mass increases the natural time periods of the structure. The damping coefficient increases marginally with the increase in the tip mass. The effect of variation of gain multiplier on active damping is also investigated. The experiments validate the relation between the gain multiplier and the active damping coefficient. However, due to hardware deficiencies a more predominant damping could not be achieved due to the use of softer PVDF and plastic materials that have high material damping. A stiffer piezoelectric material would let us use materials with lower material damping. That is the direction of future research.

References

[1] Barboni, R., Mannini, A., Fantini, E. and Gaudenzi, P., 2000, Optimal placement of PZT actuators for the control of beam dynamics. *Smart Materials and Structures*, **9**, 110–120.
[2] Lee, C.K. and Moon, F.C., 1990, Modal sensors/actuators. *Transactions of ASME*, **57**, 434–441.
[3] Seeley, C.E. and Chattopadhyay, A., 1993, The development of an optimization procedure for the design of intelligent structures. *Smart Materials and Structures*, **2**, 135–146.
[4] Onoda, J. and Hanawa, Y., 1993, Actuator placement optimization by genetic and improved simulated annealing algorithms. *AIAA Journal*, **31**(6), 1167–1169.
[5] Ryou, J.K., Park, K.Y. and Kim, S.J., 1998, Electrode pattern design of piezoelectric sensors and actuators using genetic algorithms. *AIAA Journal*, **36**(2), 227–233.
[6] Saha Chaudhuri, A., 2003, Piezolaminated structures with large deformations, PhD Thesis, Indian Institute of Technology, Bombay, India.